



Energy-economic analysis and optimization of a shell and tube heat exchanger using a multi-objective heat transfer search algorithm

Parth Prajapati ^a, Bansi D. Raja ^b, Vivek Patel ^a, Hussam Jouhara ^{c,d}

^a Department of Mechanical Engineering, Pandit Deendayal Energy University, Gandhinagar 382421, Gujarat, India

^b Department of Mechanical Engineering, Indus University, Ahmedabad, Gujarat, India

^c Heat Pipe and Thermal Management Research Group, College of Engineering, Design and Physical Sciences, Brunel University London, UBS 3PH, UK

^d Vytautas Magnus University, Studentu Str. 11, LT-53362 Akademija, Kaunas Distr., Lithuania

ARTICLE INFO

Keywords:

Energy-economic analysis
Optimization
Shell and tube heat exchanger
Heat transfer search algorithm
Parametric analysis

ABSTRACT

This study presents the energy-economic analysis and optimization of a shell and tube heat exchanger. A water-water, segmental baffled shell and tube heat exchanger was designed using the Kern method and analysed by performing energy and economic modelling. The analysis is carried out considering the design variables on the shell side i.e. baffle cut, baffle spacing, shell diameter and tube side variables i.e. tube layout, tube outside diameter, number of tube passes and number of tubes. The multi-objective heat transfer search algorithm was used to optimize the heat exchanger for minimum total cost and maximum heat exchanger efficiency. Multiple optimal solutions were presented using the Pareto optimal curve. TOPSIS selection criteria was used to identify the optimum operating condition. Within the given bounds of the variables, the shell and tube heat exchanger can be operated at a minimum cost of 72,000 \$/year resulting in 16.4 % efficiency, or, it can be operated at a maximum efficiency of 81.6 % with a total cost of 275,000 \$/year. The scattered distribution of shell diameter, baffle spacing, number of tube passes and number of tubes between the lower and upper bound represent their substantial role in optimizing the heat exchanger performance. The number of tubes and tube passes showed the maximum variation in efficiency, while significantly less impact was observed when the tube layout was altered.

1. Introduction

Heat exchangers are associated with almost every industry, primarily in energy generation and heat exchange in general. It is observed that energy demands are increasing at a rapid rate. Also, with growing industries and sustainable development required, it has become inevitable to optimize such systems in a manner to increase output at a lower cost and lower energy consumption [1–3]. Generally, according to the application, an industry uses shell and tube heat exchangers (STHE), gasketed plate heat exchangers (PHE), finned-surface heat exchangers, and double-pipe heat exchangers [4]. However, the most widely used heat exchanger is the shell and tube heat exchanger due to its simple design, higher heat transfer, and reliability at high pressures [5,6]. It is used when fluid quantities, fluid flow rates, and pressures are high. Thus, optimizing STHEs will be very helpful to many industries. In an STHE, several design parameters affect the system's thermodynamic performance. Thermodynamic performance refers to heat transfer rate, heat losses, entropy generation, effectiveness, and pressure drop. Apart from thermodynamic performance, we should also focus on economics.

Thus, the main objectives of the current work are to optimize the thermodynamic performance and to decrease the overall cost of an STHE by optimizing the operational and geometrical parameters.

Many researchers have contributed to the optimization of heat exchangers with different methodologies and approaches. Mehdi et al. [7] optimized STHEs by adding helical circular grooves of different depths and then selected an optimum depth, increasing the heat transfer rate by ~5 % with a very minute variation in pressure drop. According to the Bell-Delaware method, Medardo et al. [8] used a Genetic algorithm (GA) to find the design parameter's optimum value. Sadegzadeh et al. [9] considered cost as the objective function and minimized it using the GA and particle swarm optimization algorithm. Hajabdollahi et al. [10,11] analysed STHEs and gasket-plate heat exchangers from an economic standpoint. They reduced the total cost of STHEs by ~35 % and gasket-plate heat exchangers by ~13 %. They used a multi-objective optimization through NSGA-II and performed the exergy analysis to observe the performance parameters simultaneously. Mohanty [12] used a gravitational search algorithm based on the law of gravity and mass interactions to optimize the STHE from an economic perspective. Dhavle et al. [13] performed a design and economic optimization of STHEs

E-mail addresses: vivekp@sot.pdpu.ac.in (V. Patel), Hussam.Jouhara@brunel.ac.uk (H. Jouhara).

<https://doi.org/10.1016/j.tsep.2024.103021>

Received 25 April 2024; Received in revised form 25 September 2024; Accepted 27 October 2024

Available online 30 October 2024

2451-9049/© 2024 The Author(s). Published by Elsevier Ltd. This is an open access article under the CC BY license (<http://creativecommons.org/licenses/by/4.0/>).

Nomenclature		Re	Reynolds number
A	heat transfer area, m ²	Nu	Nusselts number
B _C	Baffle cut, %	b _o	Boiling number
B _S	Baffle spacing	<i>Greek symbols</i>	
D _S	Shell Diameter	η _{HE}	heat exchangers efficiency
D _t	Tube outside diameter	η _{ex}	exergetic efficiency
D _{eq}	equivalent diameter	η _P	Pump efficiency
L _{BB}	Bypass channel diametral gap	Φ	tube layout
t _b	Baffle thickness, m	<i>Abbreviations</i>	
L _{tb}	Diametral tube-to-baffle clearance, m	E _D ^{AV}	Avoidable part of exergy destruction
L _{sb}	Diametral shell-to-baffle clearance, m	CAPC	Capital Cost of investment
L _t	Length of the tube, m	CEPCI	Chemical engineering plant cost index
R _f	fouling resistance, m ² K/W	C _{index}	Cost index factor
Ex	exergy	EN	Endogenous part of exergy destruction
h	heat transfer coefficient	EX	Exogenous part of exergy destruction
U	overall heat transfer coefficient	GA	Genetic Algorithm
ṁ	mass flow rate, kg/s	HE	Heat Exchanger
N _P	Number of tube pass	HTSA	Heat transfer search algorithm
ΔP	pressure drop, kPa	OPC	Operational Cost
t	tube side	SS	Stainless steel
s	shell side	STHE	Shell and tube heat exchanger
i	inlet	UN	Unavoidable part of exergy destruction
o	outlet	XD	Total exergy destruction
PP	pumping power, kW		
W	work done		

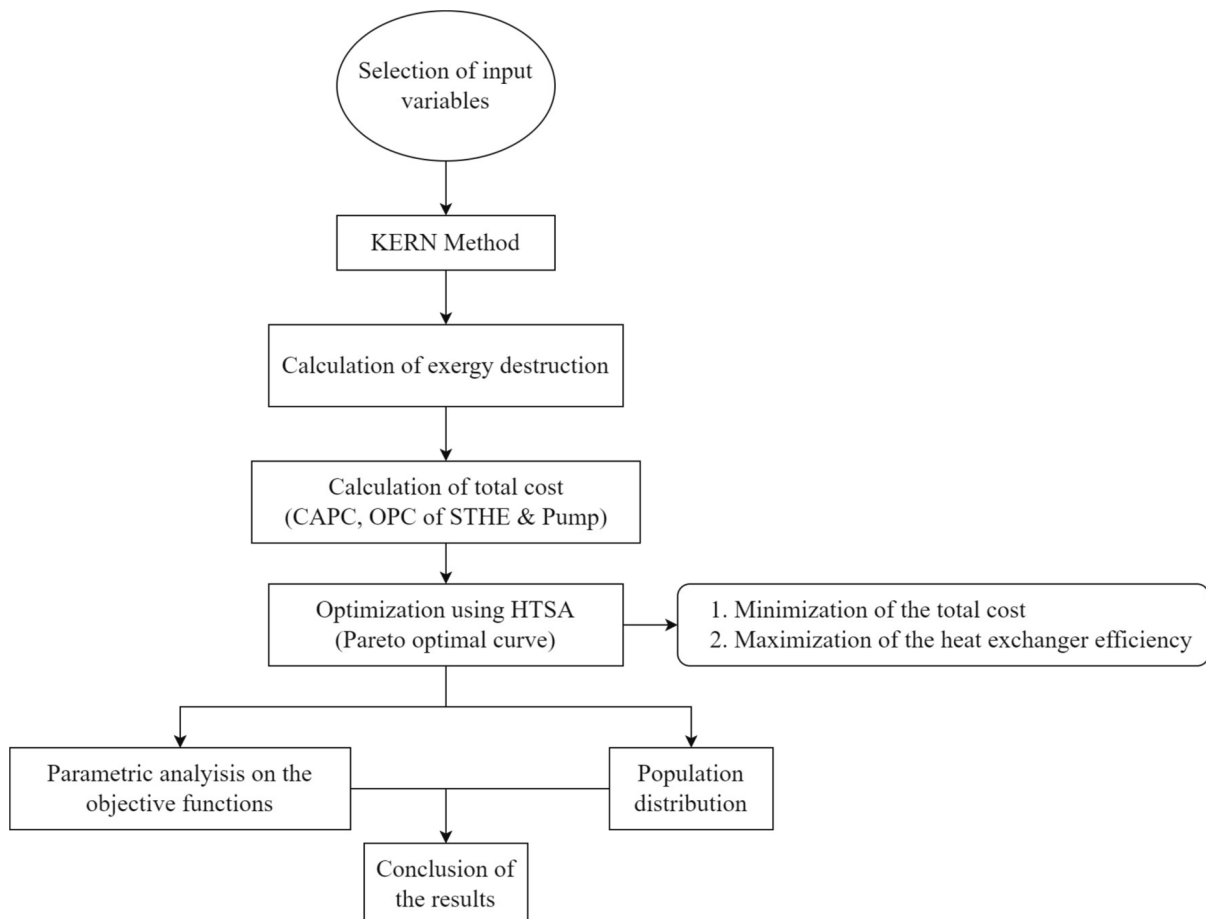


Fig. 1. Methodology of the design and optimization process of the STHE.

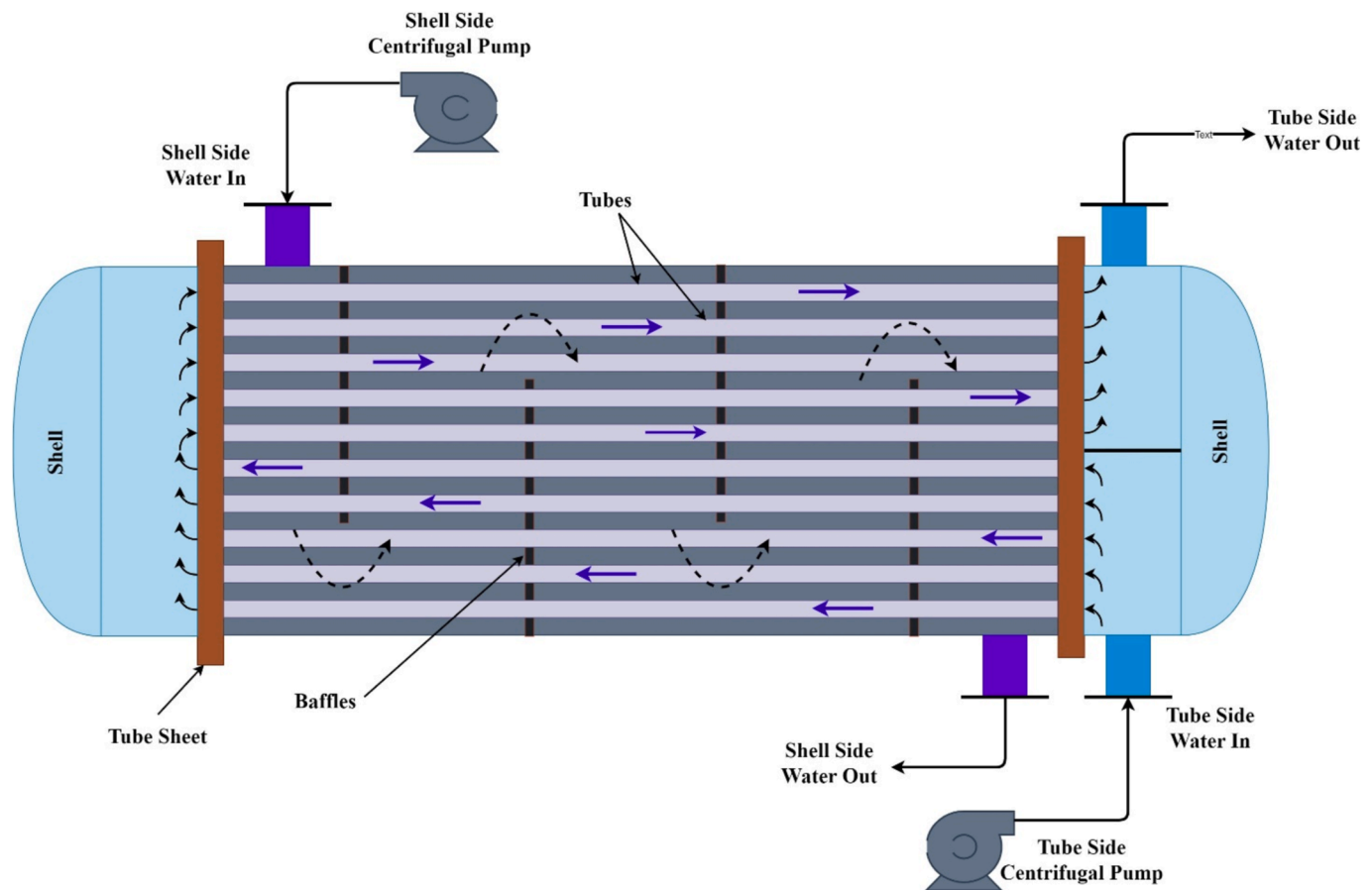


Fig. 2. Shell and tube heat exchanger arrangement.

using a cohort intelligence algorithm. The effect of parameters like tube outside diameter, baffle space, pitch size, shell diameter and number of tubes on the total cost of the heat exchanger was studied.

In a study carried out by Wang et al. [14], the influence of corrugation parameters on thermal-hydraulic performance of the STHE was studied. It was observed that the maximum heat transfer efficiency was obtained at a corrugation angle of $\beta = 60^\circ$. Han et al. [15] used an improved sparrow search algorithm to perform a thermal-economic optimization design of STHE. The study focussed on constructing a thermal-economical model using the Kern and Bell-Delaware method and proposed a novel mechanism to obtain an optimized design of the heat exchanger. Caputo et al. [16] identified a research gap wherein concluded that the choice of an objective function strongly affects the optimal design of the heat exchanger.

Bicer et al. [17] used computational fluid dynamics and the Taguchi method to optimize the design of the STHE with a novel three-zonal baffle. Thondiyil and Kizhakke [18] used the Taguchi method to carry out the optimization of shell and tube heat exchangers with staggered baffles. Computational fluid dynamics was used to simulate the system and consider different parameters and geometries. A maximum heat transfer rate of 141 kW could be achieved with the optimum combination. Khosravi et al. [19] used a Genetic algorithm (GA), firefly algorithm (FA) and cuckoo search (CS) method to maximize the thermal efficiency of the STHE. The effect of seven key variables on the efficiency of the heat exchanger was studied and optimized. Saldanha et al. [20] analysed the performance of different evolutionary algorithms like Predator-Prey, Multiobjective particle swarm optimization and NSGA II with the objective of of minization of heat transfer area and pumping power in a shell and tube heat exchanger. In a study done by Mohapatra et al. [21], an optimal plate-fin heat exchanger design optimization is studied using opposition-based orthogonal learning kho-kho

optimization algorithm. The issues addressed during the optimization study were total weight, number of entropy generation units and total annual costs.

Along with costs, researchers also considered performance optimization based on exergy. Such a combination of optimization studies is known as 'exergo-economic optimization'. Muhammad et al. [22] performed an exergo-economic analysis of an STHE using the methods of Kern, Bell-Delaware, and Wills-Johnston and compared the results of all these methods. They also optimized the system using GA, and the results showed that the Bell-Delaware and Will-Johnston methods gave similar values. In contrast, results through the Kern method deviated significantly. After optimization, the heat transfer area was reduced by 26.4 %, capital cost by 20 %, and operational cost by 22 %. Li et al. [23] analysed the thermal-hydraulic performance and determined the energy efficiency of STHES. The numerical investigation was conducted for heat transfer enhancement.

The objectives of this study are: (i) To design an STHE using the 'Kern' method, perform the energy analysis, and find the total amount of exergy destruction (ii) to perform an economic analysis to find the variation of the total cost associated with various parameters of STHE (iii) Optimizing the system with the help of the Heat Transfer Search Algorithm (HTSA) by obtaining the Pareto front of the total cost and heat exchanger efficiency and then selecting the optimum point from the Pareto front (iv) Perform the parametric analysis of different design variables to observe the sensitivity/impact of that parameter against heat exchanger efficiency and cost.

Section 2 describes the methodology for this work as shown in Fig. 1. Section 3 describes the system configuration and various types of modelling, i.e., thermal, exergy, and economic modelling, with their essential correlations for the Kern method. At the end of the section, the formulation of the objective function is given. Section 4 explains the

Table 1
Geometric configuration of the STHE [22,25].

Parameters	Value
Mass flow rate shell, kg/s	27.80
Mass flow rate tube, kg/s	68.90
Shell side temperature outlet, °C	40
Shell side temperature inlet, °C	95
Tube side temperature inlet, °C	25
Tube side temperature outlet, °C	40
Fouling resistance, R_f shell, $m^2.K/W$	0.00034
Fouling resistance, R_f /tube, $m^2.K/W$	0.00020
Length of the tube (L_t), m	4.83
Number of pair of sealing strips, N_{ss}	2
Diametral shell-to-baffle clearance, L_{sb} , m	0.0051
Diametral tube-to-baffle clearance, L_{tb} , m	0.0008
Baffle thickness, t_b , m	0.005
Bypass channel diametral gap, L_{bb} , m	0.019
Allowable pressure drop of tube and shell side, P_t , kPa	100

heat transfer search algorithm used to optimize the system. Section 5 shows the results after the optimization and parametric analysis. Section 6 showcases the important findings and the conclusion of the work.

2. Methodology

This study aims to design a shell and tube heat exchanger using the 'Kern Method' with the help of the Matlab code and to generate results as in [22], then performing various analyses: Energy, economic, heat transfer analysis, and the optimization of the system with the help of the HTS algorithm. The HTS algorithm provides multiple optimal solutions represented on a Pareto front and selects the optimum value from those set points of values. TOPSIS selection criteria which is one of the multi-criteria decision-making techniques, is employed to select an optimal point among multiple optimal solutions.

A parametric analysis is carried out on design variables on the shell side that includes, shell diameter, baffle spacing and baffle cut. Similarly, the design variables on the tube side are tube outside diameter, tube layout, number of tubes, and number of tube passes. The steps involved in the methodology of design and optimization of the STHE are presented using a detailed flowchart in Fig. 1.

3. System description and thermo-economic modeling

3.1. System configuration

The system comprises one STHE and two centrifugal pumps at shell and tube side inlets. The heat exchanger is liquid phase water-water with segmental baffles. The flow in the shell side is cross-flow. The pumps are used to counterbalance the pressure drops in the heat exchanger and maintain the pressures inside the HEX as shown in Fig. 2. In the current study, the required data for the analysis are chosen from [22] and given in Table 1. The water pressures at the shell and tube side outlets are 1.5 bar and 1 bar, respectively. The heat transfer rate for the considered design of shell and tube heat exchanger is 4.2 MJ. The other values of the configuration are calculated according to the design method adopted. There are many STHE design methods, however, for the current study, the Kern method is used [24].

3.2. Thermo-economic modelling

The thermo-economic modelling of a shell and tube heat exchanger involves calculating tube and shell side parameters separately. Some of the parameters involved are Reynolds number (Re), Nusselt number (Nu), heat transfer coefficient (h), pressure drop (ΔP), overall heat transfer coefficient (U), and correction factors of shell side pressure drop. The economic parameters such as pumping power (PP), cost index factor (C_{index}), operational cost (OPC), and capital cost (CAPC) are

Table 2
Constraints for the design parameters [22].

No.	Parameters	Lower bound	Upper bound
1	Layout, degrees	30°	90°
2	Shell diameter, mm	100	1500
3	Tube outside diameter, mm	15	51
4	Baffle cut, %	20	35
5	Baffle spacing, mm	50	500
6	Number of tube passes	1	8
8	Number of tubes	900	2000

calculated for both pumps and the heat exchanger.

It is important to note that an STHE is designed in two phases. The first phase is designing the tube side, and the second is designing the shell side. The calculations for the tube side variables are elementary. In contrast, the shell side design is more complicated because it accounts for different and variable geometric parameters like tube layout, baffle spacing, baffle cut, number of baffles, bundle diameters, and various clearances. Thus, for all the methods available for designing the STHE, the tube side calculations remain the same, while only the shell side calculations are changed in every technique. All the calculations were made on MATLAB software. Apart from the specifications given above, lower and upper bounds of the parameters were also required, as mentioned in Table 2.

Various correlations for the Kern method are,

$$Re_t = \frac{\rho_t \vartheta_t D_t}{\mu_t} \quad (1)$$

$$t = \frac{(t_{in} + t_{out})}{2} \quad (2)$$

If $Re_t < 2300$ then the Nusselt number can be found from

$$Nu_t = \frac{h_t k_t}{d_i} = \frac{k_t}{d_i} = \left[3.657 + \frac{0.0677 (Re_t Pr_t d_i / L)^{1.33}}{1 + 0.1 Pr_t (Re_t d_i / L)^{0.33}} \right] \quad (3)$$

If $2300 < Re_t < 10000$ then the Nusselt number can be found from

$$Nu_t = \frac{h_t k_t}{d_i} = \frac{k_t}{d_i} = \left[\frac{(ft/8)(Re_t - 1000) Pr_t}{1 + 12.7(ft/8)^{0.5} (Pr_t^{2/3} - 1)} (1 + d_i/L)^{0.67} \right] \quad (4)$$

where, $f_t = (1.82 \log_{10} Re_t 1.64)^{-2}$.

If $Re_t > 10000$ then the Nusselt number can be found from

$$Nu_t = \frac{h_t k_t}{d_i} = \frac{k_t}{d_i} = 0.027 k_t / d_o Re_t^{0.8} Pr_t^{0.33} \quad (5)$$

$$Pr_t = \frac{\mu C_p}{k} \quad (6)$$

$$h_t = \frac{\rho_t (1.35 + 0.02t) \vartheta_t}{(1000D_t)^2} \quad (7)$$

$$\Delta P_t = \frac{\rho_t \vartheta_t^2 \left[\left(\frac{L f_t}{D_t} \right) + P_c \right] N_p}{2} \quad (8)$$

$$P_c = 2.5$$

$$Re_s = \frac{G_s D_{eq}}{\mu_s} \quad (9)$$

$$h_s = j_h k_s Re_s \left(\frac{Pr_s^{0.33}}{D_{eq}} \right) \quad (10)$$

$$f_s = 2b_o Re_s^{-0.15} \quad (11)$$

$$\Delta P_s = \rho_s g_s^2 f_s \frac{L_t D_s}{2 B_s D_{eq}} \quad (12)$$

where the value b_0 is considered to be 0.72, according to Peters and Timmerhaus [26].

3.3. Exergy modeling

Exergy is the amount of energy released/transferred from a substance until it reaches thermal and chemical equilibrium with the surroundings. For example, the temperature of a cup of tea is 80 °C, and it is put open to the environment at 25 °C. The total amount of energy that is transferred from tea to the environment until it reaches 25 °C is the amount of exergy that hot tea possesses. A hot stream always enters through the shell side inlet, and the temperature of the stream gradually decreases and the density increases. This helps that stream move downwards to be released from the shell side outlet at the bottom.

The cold stream is continuously pumped through the tubes that absorb energy and its temperature increases, leading to a decrease in density which facilitates upward movement [27].

The formula to find the exergy is:

$$Ex = [(h_1 - h_0) - T_0(s_1 - s_0)] \quad (13)$$

Here, h and s represent the enthalpy and entropy of the substance/fluid. h_1 represents enthalpy at temperature 1, i.e., the initial temperature of the substance, and s_1 represents initial entropy at temperature 1. T_0 is the environment/ambient temperature at which the substance will reach equilibrium. h_0 and s_0 are the enthalpy and entropy at the dead state [28–30]. A system is said to be in thermal and chemical equilibrium with the surroundings, with no possibility of heat transfer [27]. For the present case, the hot and cold streams possess the exergy. In addition, the energy provided to the streams by the pumps and the power required by the pump are also considered for exergy calculations. The exergy can be calculated as [31]

$$Ex_{hot} = [(h_1 - h_0) - T_0(s_1 - s_0)] \dot{m}_s \quad (14)$$

$$Ex_{cold} = [(h_2 - h_0) - T_0(s_2 - s_0)] \dot{m}_t \quad (15)$$

The power required by the pumps is,

$$PP_t = \frac{\dot{m}_t \Delta P_t}{\eta_p} \quad (16)$$

$$PP_s = \frac{\dot{m}_s \Delta P_s}{\eta_p} \quad (17)$$

$$PP = PP_t + PP_s \quad (18)$$

where η_p is pump efficiency, and both pumps have 70 % efficiency.

There is a term called “Exergy Destruction” for finding exergy losses. It refers to the irreversibilities associated with the system, like surface friction, fouling resistance, pressure drop, etc. The difference of exergies at the inlet and exit of the HE gives exergy that has been destroyed [32].

$$X_{D,STHE} = Ex_{c,i} + Ex_{H,i} - Ex_{C,o} - Ex_{H,o} \quad (19)$$

$$X_{D,P} = Ex_{P,i} + W - Ex_{P,o} \quad (20)$$

$$XD = X_{D,STHE} + X_{D,P} \quad (21)$$

Here $X_{D,STHE}$ is the total amount of exergy destruction by STHE and $X_{D,P}$ is the total exergy destruction by both pumps. Combining both of these will result in total exergy destruction (XD).

3.4. Economic modelling

The system consists of two components: an STHE and two centrifugal

pumps. The economic analysis of the system will include both components. The cost of any component comprises capital cost (CAPC) and operational cost (OPC) [9,33,34]. Capital cost is the total investment cost for purchasing the component, and OPC is all the other costs laid when the system works (such as the cost of electricity). The steps for calculating all of these costs are explained in the subsequent section.

3.4.1. Capital cost

The capital cost of any component depends upon component material, time of purchase, supplier, and product quality [35]. In our case, the material of the HEX is SS-SS (Shell side – tube side). Many researchers have developed direct correlations for finding the capital cost by considering the principal design parameters for different types and materials of the heat exchanger. As they are not considering every dimension of the HE, we can only get a reasonable estimate of the cost associated with the capital investment. The correlation in this study is taken from [36].

$$CAPC_{HE} = 8000 + 259.2A^{0.91} \quad (22)$$

where A is the heat transfer area (m^2). Similarly, the capital cost of centrifugal pumps can be calculated as [37],

$$CAPC_{pump} = 13.92 \dot{m}_w \Delta P^{0.55} \left(\frac{\eta_p}{1 - \eta_p} \right)^{1.05} \quad (23)$$

The C_{index} is calculated by taking the value of CEPCI of the current year and a reference year. The reference year is 1990, the current year is 2020, and their CEPCI values are 390 [21] and 650 [22].

$$C_{index} = \frac{CEPCI_{current}}{CEPCI_{reference}} \quad (24)$$

The cost index for the present study is,

$$C_{index} = \frac{650}{390} \approx 1.7 \quad (25)$$

Therefore, the current cost of any component can be given as,

$$CAPC_{current} = C_{index} \times CAPC_{reference} \quad (26)$$

3.4.2. Operational cost

The OPC is the cost while the equipment is operating. It depends on equipment life n_y (in years), annual cost C_o (\$/year), price of unit electricity $C_{electricity}$ (\$/kWh), operating hours availability Λ (hours), annual inflation rate i (%), and pumping power. To calculate OPC,

$$OPC = \sum_{j=1}^{n_y} \frac{C_o}{(1+i)^j} \quad (27)$$

$$C_o = PP \times C_{electricity} \times \Lambda \quad (28)$$

The values of the other parameters considered are $n_y = 10$ years, $\Lambda = 7000$ h/year, $C_{electricity} = 0.12$ \$/kWh, and $i = 10$ % [34].

3.5. Objective function formulation and decision variables

The current study involves an energy economic analysis and optimization of an STHE. The optimization is associated with the minimization of total cost and maximization of heat exchanger efficiency. The thermo-economic optimization is performed with the help of a heat transfer search algorithm. Thus, the objective function for optimization can be formulated as,

$$\text{Maximize/Minimize } f(X) = f_1(X), f_2(X) \quad (29)$$

$$X = [x_1, x_2, \dots, x_k] \quad (30)$$

where $f_1(X)$ and $f_2(X)$ represent heat exchanger efficiency and total cost, respectively, and X indicates the value of various decision variables,

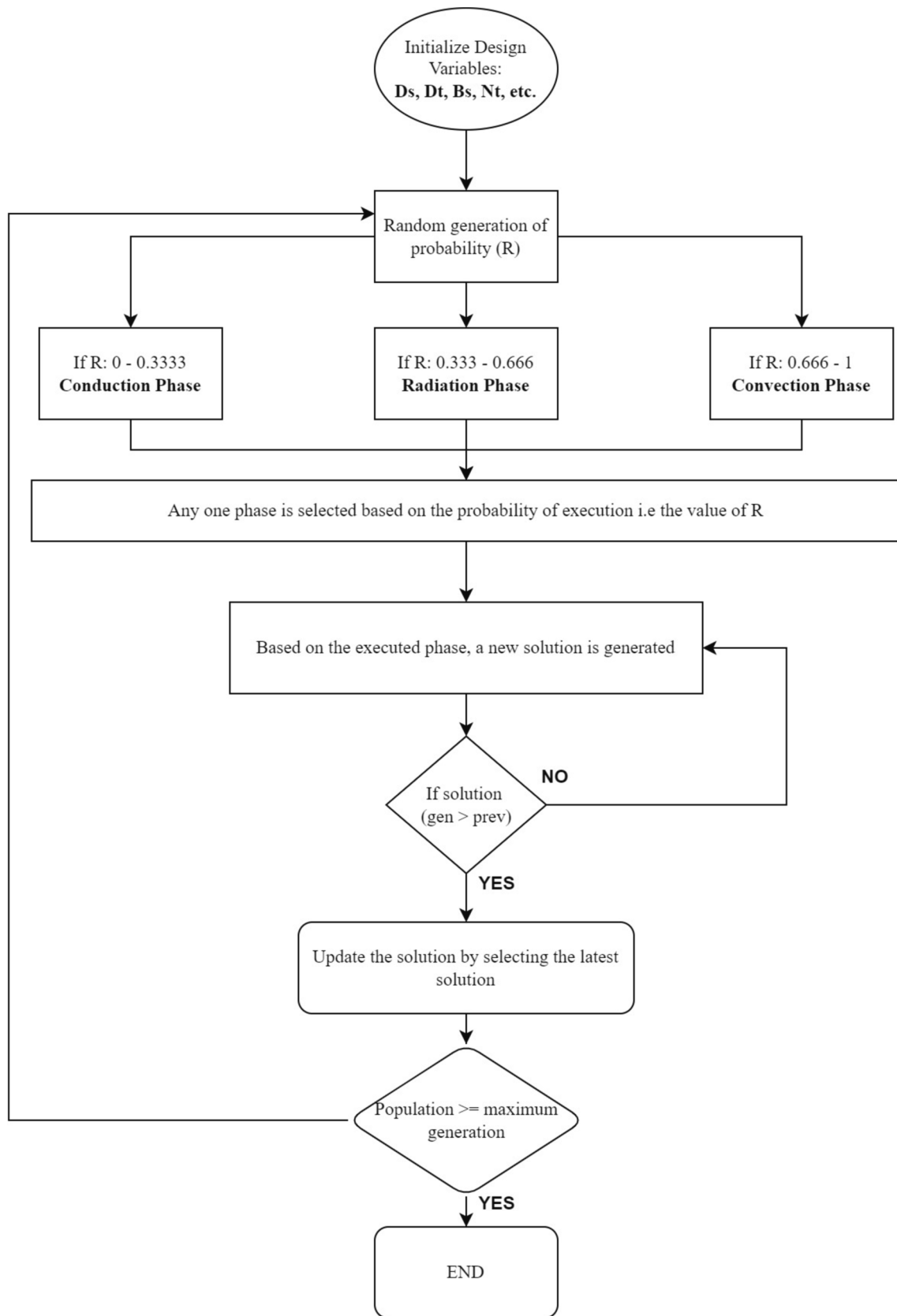


Fig. 3. Flow chart of heat transfer search algorithm.

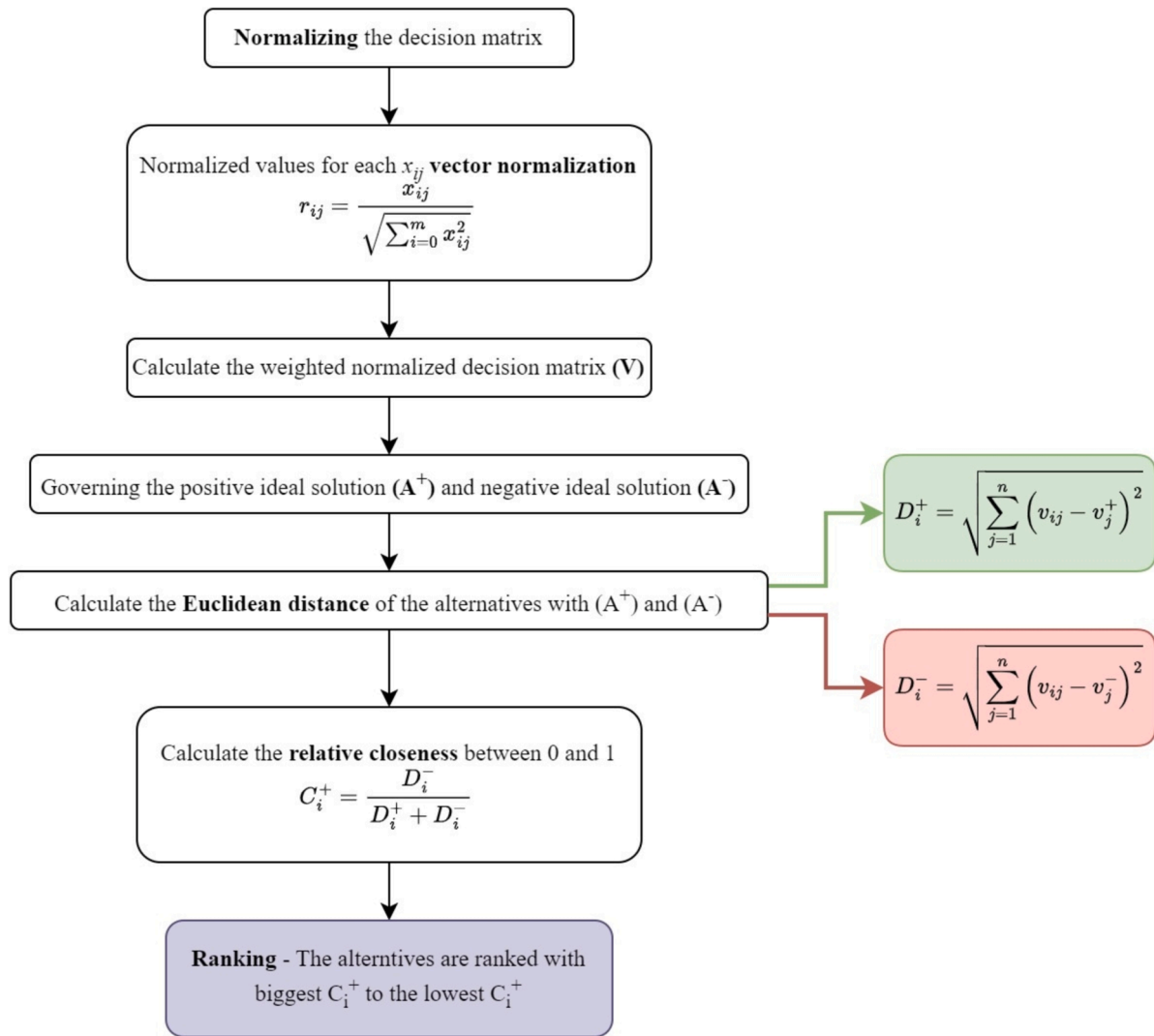


Fig. 4. Flowchart of TOPSIS decision-making.

which decides the objective function values.

In the present work, there are a total of seven decision variables: tube layout (Φ), shell diameter (D_S), tube outside diameter (D_T), baffle spacing (B_S), baffle cut (B_C), number of tube passes (N_P) and number of tubes (N_T). The upper and lower bounds of all these variables are given in Table 2. The optimization algorithm is explained in the next section.

4. Heat transfer search algorithm and TOPSIS selection criteria

Heat transfer search (HTS) is a metaheuristic optimization algorithm developed in 2015 [38]. The algorithm is developed by taking the natural laws of thermodynamics and heat transfer as the base. According to the fundamental laws of thermodynamics, any system always tries to be in thermal equilibrium with its surroundings by absorbing or releasing energy, which follows the laws of heat transfer. The heat can be transferred in three ways: conduction, convection, or radiation. Similarly, the HTS algorithm comprises three phases, i.e., conduction, radiation, and convection.

HTS is a population-based algorithm that starts by optimizing an initial solution until the global optimum point is reached. In the process, only better points are selected than the previous ones, i.e., incorporating the greedy selection process. In nature, heat is transferred by the interaction between the molecules of the system and the surroundings, where the temperature of the molecules determines the amount of

energy present in them. The same analogy is observed in this algorithm. The algorithm is composed of a population (like a system comprised of molecules), where the value of decision variables determines the value of the objective function (like temperatures of molecules determine the amount of energy present in them). All three phases in this algorithm have an equal probability of execution during the optimization, i.e., each phase has a probability of 33 %.

The algorithm starts with generating the initial values of the objective with function with the help of assigned decision variables (say $i = 1, 2, 3, \dots, m$). Then, a whole population (say $j = 1, 2, 3, \dots, n$) is generated for the updated results through a predefined number of generations (N_g) with the help of any of the 3 phases. The detailed process flowchart of the optimization algorithm is presented in Fig. 3.

4.1. Conduction phase

The conduction heat transfer occurs between molecules with a higher and lower magnitude of energy. It is imitated in the HTS algorithm during the conduction phase. The energy levels are analogous to the objective function values. The objective function value is calculated based on the initial random population, and the solutions (objective function value) are updated using Eqs. (31) and (32).

$$y_{j,i}' = \begin{cases} y_{k,i} + \left(-R^2 y_{k,i} \right), \text{iff} (y_j) > f(y_k) \\ y_{j,i} + \left(-R^2 y_{j,i} \right), \text{iff} (y_j) < f(y_k) \end{cases}; \text{if } N_g \leq N_{g,max}/C_d F \quad (31)$$

$$y_{j,i}' = \begin{cases} y_{k,i} + \left(-r_i y_{k,i} \right), \text{iff} (y_j) > f(y_k) \\ y_{j,i} + \left(-r_i y_{j,i} \right), \text{iff} (y_j) < f(y_k) \end{cases}; \text{if } N_g > N_{g,max}/C_d F \quad (32)$$

where, $y_{j,i}'$ indicates the updated solution and $C_d F$ is the conduction factor. R indicates the probability for this phase and is taken randomly from 0 to 0.3333. r_i is the random number between 0 and 1, which is uniformly distributed. $N_{g,max}$ denotes the maximum number of generations. In this phase, a random solution is selected from the population, and if the solution is better than the previous one, it is selected, or another solution is found.

4.2. Convection phase

The convection phase represents the convection heat transfer between the system and surroundings using Newton's law of cooling. Similarly, the better point is selected while comparing it with the mean solution of the population. Mathematically, it can be represented as,

$$y_{j,i}' = y_{j,i} + R(y_s - T_c F^* y_{ms}) \quad (33)$$

$$TCF = \begin{cases} \text{abs}(R - r_i), \text{if } N_g \leq N_{g,max}/C_o F \\ \text{round}(1 + r_i) + \left(-R^2 y_{j,i} \right), \text{if } N_g > N_{g,max}/C_o F \end{cases} \quad (34)$$

where $C_o F$ is the convection factor, R denoting the probability ranging from 0.6666 to 1. r_i is the random number between 0–1 distributed uniformly. y_s indicates the best solution, y_{ms} indicates the mean solution, and $T_c F$ is the temperature change factor.

4.3. Radiation phase

Stephan Boltzman's law represents the heat transfer between the surroundings and the system by thermal radiation. In the radiation mode, the solutions are selected randomly from the population and are updated according to the equations,

$$y_{j,i}' = \begin{cases} y_{j,i} + R(y_{k,i} - y_{j,i}), \text{iff} (y_j) > f(y_k) \\ y_{j,i} + R(y_{j,i} - y_{k,i}), \text{iff} (y_j) < f(y_k) \end{cases}; \text{if } N_g \leq N_{g,max}/R_d F \quad (35)$$

$$y_{j,i}' = \begin{cases} y_{j,i} + r_i(y_{k,i} - y_{j,i}), \text{iff} (y_j) > f(y_k) \\ y_{j,i} + r_i(y_{j,i} - y_{k,i}), \text{iff} (y_j) < f(y_k) \end{cases}; \text{if } N_g > N_{g,max}/R_d F \quad (36)$$

where $R_d F$ denotes the radiation mode, and R indicates the probability varying from 0.3333 to 0.6666.

The multi-objective heat transfer search (MOHTS) algorithm considers multiple objective functions simultaneously for optimizing and generating the population. The non-dominated sorting heat transfer search (NSHTS) algorithm stores the non-dominated solution generated by MOHTS. The dominated solutions are checked by ϵ -dominance and are used to update the solutions and generate the Pareto points and Pareto front. The details for the entire method are given in references [39,40].

4.4. TOPSIS criteria

The TOPSIS (Technique for Order Preference by Similarity to Ideal Solution) selection criteria is an efficient multi-criteria decision-making technique developed by Hwang and Yoon [41] to select an ideal solution among multiple optimal solutions. The selection criteria works on the principle of selecting of ideal solution that has the shortest distance to the positive ideal solution (A^+) and farthest distance from the negative

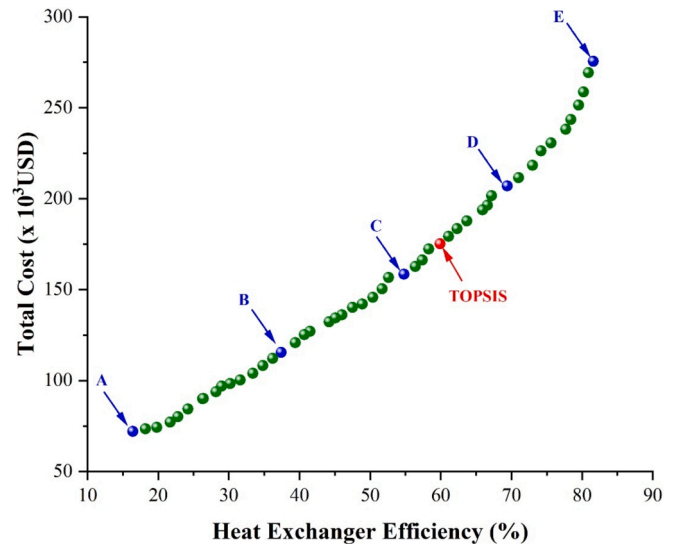


Fig. 5. Pareto front for cost and heat exchanger efficiency.

ideal solution (A^-) [42].

The stepwise procedure to select an ideal solution among the multiple optimal solutions is presented with the help of a flow-chart in Fig. 4 and explained below.

Step 1: Initially, an evaluation decision matrix is formed based on the pre-collected numerical data that comprises of options and criteria. Based on the desirability a variable is assigned as either a benefit criterion or a cost criterion.

Step 2: In this step, the performance of each variable is assessed and normalized. It is to ensure that the criteria considered for the selection are on the same scale of comparison.

Step 3: In this step, the weights are assigned to the variables based on their relative importance and it signifies their relevance/importance in the decision making process. It is equally important to understand the relative importance of criteria.

Step 4: Calculation of positive ideal solution (A^+) and negative ideal solution (A^-). The best performance is identified by the most positive ideal solution and the worst performance is identified by the most ideal negative solution. Based on the maximum and minimum values of each criteria, the solutions are identified.

Step 5: Calculation of proximity ratio based on the Euclidean distance of each variable from the ideal solution (D_i^+ and D_i^-) is carried out in this step.

Step 6: To consider all the variables on a common scale, relative closeness (proximity ratio) between 0 and 1 is calculated towards the ideal solution.

Step 7: Ranking the options in the decreasing order of relative closeness. The variables with higher proximity ratios are more desirable solutions and closer to the ideal solution. Whereas the variables with lower proximity ratios are considered to be less desired solutions.

5. Case study and results-discussion

In this study, a water-water STHE was designed using the Kern method, and based on the design parameters, an energy-economic analysis was carried out using MATLAB. The system comprised a segmental baffled shell and tube heat exchanger and two centrifugal pumps. The parameters affecting the geometric configuration of the heat exchanger are mentioned in Table 1, and the constraints for decision variables of the shell and tube side are given in Table 2. Analysis was carried out by calculating the heat exchanger efficiency, total cost and exergy destruction associated with the system. The designed heat exchanger was optimized for maximum efficiency and minimum total

Table 3
Sample design points of decision variables for cost and HE efficiency.

Points	A	B	C	D	E	TOPSIS
Tube layout	45	30	30	30	30	30
Shell diameter, D_s (mm)	1500	719	754	979	1500	883
Tube diameter, D_t (mm)	15	15.2	16.2	21.3	33	18.6
Baffle cut, B_c (%)	20.0	20.4	20.9	20.7	20	20.2
Baffle spacing, B_s (mm)	500	445	417	254	162	333
Number of tube pass, N_p	1	2	4	7	8	5
Number of tubes, N_t	900	115.5	2000	2000	2000	1957
Total cost (10^3 \$)	72.1	37.4	158.5	207	275.6	175.1
Heat exchanger efficiency	16.4	115.5	54.8	69.4	81.6	59.9

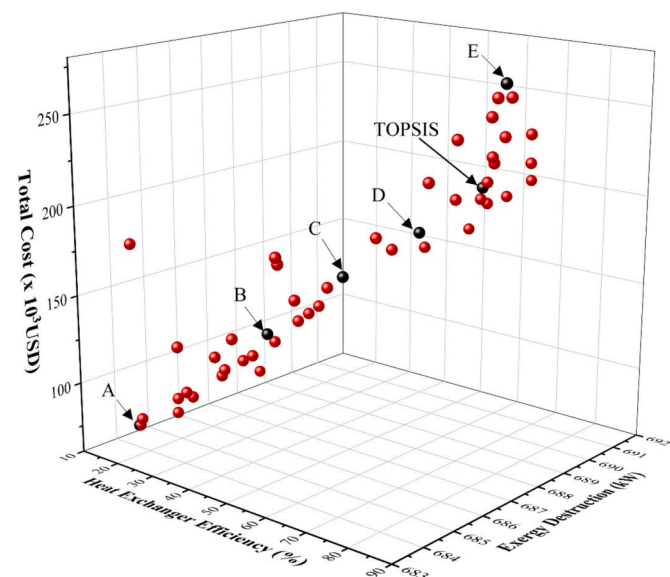


Fig. 6. Pareto optimal curve for three objective functions.

cost using a heat transfer search optimization algorithm.

The two-objective and three-objective optimization was performed for the total cost, heat exchanger efficiency and exergy destruction in the shell and tube heat exchanger. A Pareto curve was generated with multiple Pareto optimal points, each point representing a potential optimal solution. The curve shows a direct relation between the total cost and heat exchanger efficiency.

Fig. 5 shows the distribution of Pareto points for total cost per year and heat exchanger efficiency. The Pareto points A and E marked on the Pareto curve represent the condition of the minimum total cost of the heat exchanger and the maximum heat exchanger efficiency respectively. The maximum heat exchanger efficiency of 81.6 % was obtained with a total cost of 275,000 \$/year as represented by point E on the Pareto curve. Similarly, point A represents the minimum cost of the heat exchanger obtained as 72,000 \$/year when the heat exchange efficiency was just 16.4 %. Table 3 indicates the five-sample optimal points A–E as presented on the Pareto curve and signifies the value of heat exchanger efficiency and the total cost. The optimal operating condition was determined using the TOPSIS criteria for which the heat exchanger efficiency and the total cost were 59.9 % and 175,100 \$/year.

The distribution of three objective Pareto optimal points is shown in Fig. 6 for the total cost, heat exchanger efficiency, and exergy destruction in the heat exchanger. Between the extremities, the heat exchanger efficiency, total cost, and exergy destruction vary from 16.3 % to 81.6 %, 721,00 \$/year to 273,800 \$/year and 683.7 kW to 687.8 kW, respectively. The variation in the total cost and the heat exchanger is substantial, however, the exergy destruction cost variation is marginal owing to the lower operating temperature (95 °C) of water in the heat exchanger. The exergy destruction rate is subject to vary substantially

Table 4
Sample design points of decision variables for total cost, HE efficiency and exergy destruction.

Points	A	B	C	D	E	TOPSIS
Tube layout	45	45	30	30	45	30
Shell diameter, D_s (mm)	1500	1250	1230	1150	1.49	1170
Tube diameter, D_t (mm)	15	17	20	20	33	23
Baffle cut, B_c (%)	20	20	21	20	21	21
Baffle spacing, B_s (mm)	500	430	300	260	150	240
Number of tube pass, N_p	1	1	4	5	8	7
Number of tubes, N_t	900	1711	1829	1966	2000	1991
Total cost (10^3 \$)	72.1	127.1	166.4	187.1	273.8	210.3
Heat exchanger efficiency	16.3	29.6	54.1	62.2	81.6	70
Exergy destruction, kW	684.1	683.9	686.2	687.7	687.8	688.8

Table 5
Validation of the results obtained using the proposed approach.

	GA approach [19]	HTS approach
Tube side heat transfer co-efficient, (W/m ² K)	3964	3753
Shell side heat transfer co-efficient, (W/m ² K)	3110	1965
Overall heat transfer co-efficient, (W/m ² K)	789	688
Tube side pressure drop, (Pa)	3426	3422
Shell side pressure drop, (Pa)	10,168	1813
Capital cost, (\$)	69,582	69,958
Operating cost, (\$)	3878	2126
Total cost, (\$)	73,460	72,084

Table 6
Comparative results of the present approach with other optimization algorithms.

	GA	PSO	BBO	HTS
Tube layout	30	30	30	30
Shell diameter, D_s (mm)	1500	1500	1500	1500
Tube diameter, D_t (mm)	35	30	30	33
Number of tube pass, N_p	8	8	8	8
Number of tubes, N_t	1750	1845	1991	2000
Heat exchanger efficiency	79.1	80.3	81.6	81.6

high with the increase in the operating temperature and subsequent change in the geometric design of the heat exchanger.

The magnitude of the objective function for five sample optimal points A–E and the optimum operating condition as identified using the TOPSIS criterion is tabulated in Table 4. At the optimum point, the heat exchanger efficiency was 70 %, the total cost as 210,300 \$/year and the exergy destruction of 689 kW was obtained. In the subsequent section, parametric analysis is presented for the design variables on the shell and tube side.

The validation of the results obtained using the proposed approach is carried out by comparing the results of the present case study obtained using the GA and reported in the literature [22]. The comparative results are presented in Table 5. It can be observed from the results that the optimized heat exchanger design obtained using the proposed approach results in lower operating costs as compared to the GA approach. However, the capital cost of the heat exchanger design obtained using the proposed approach is marginally higher than the GA approach. Overall, the total cost of the optimized heat exchanger design obtained using the proposed approach is 1.9 % lower as compared to the previously reported design.

In order to improve the visibility of the proposed investigation, optimization algorithms such as Genetic Algorithm (GA), Particle Swarm Optimization (PSO), and Biogeography Based Optimization (BBO) are implemented in the presented case study. These algorithms are implemented for the maximum heat exchanger efficiency consideration of the presented case study. The comparative results of all these algorithms with the proposed approach are presented in Table 6. It can

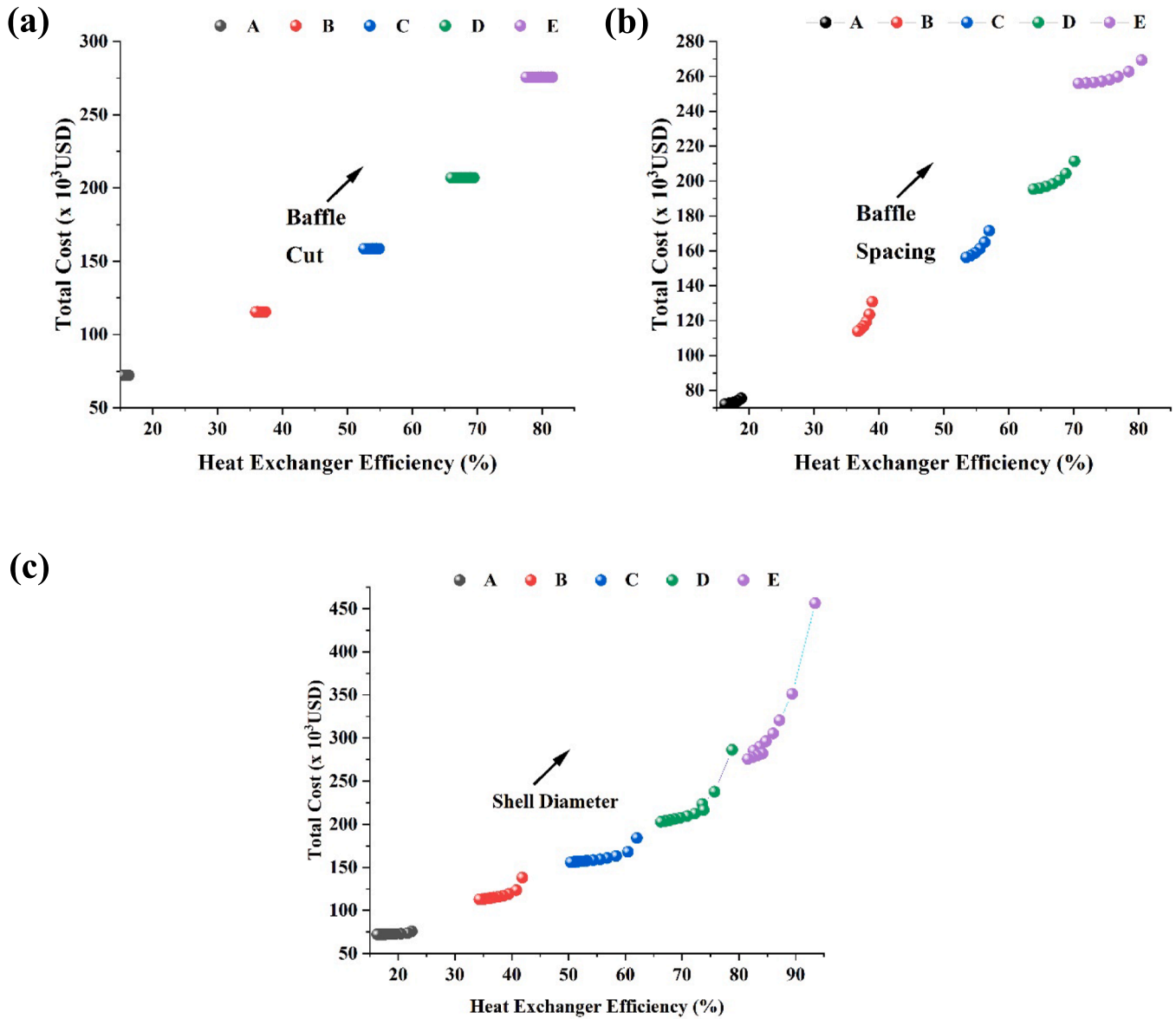


Fig. 7. Results of parametric analysis for the variables of shell side.

be observed from the results that the optimized heat exchanger design obtained using the BBO and HTS is identical in efficiency and better as compared to the GA and PSO approaches.

5.1. Parametric analysis – shell side design variables

The parametric analysis is carried out for the shell side design variables to understand the effect of baffle cut, baffle spacing and shell diameter on the heat exchanger efficiency and total cost of the system. On the Pareto curve, five sample points A–E are selected arbitrarily and for each point, the behaviour of the heat exchanger is studied and presented in Fig. 7.

With the increase in the baffle cut, baffle spacing and shell diameter, the total cost of the heat exchanger increases because of the increase in the size of the heat exchanger. At the same time, the heat exchanger efficiency increases resulting from increased heat transfer rates and lower pressure drops allowing the fluid to flow smoothly. The effect of increasing the geometrical design variable on the shell side is most profound for the shell diameter as shown in Fig. 7(c). The maximum heat

exchanger efficiency of 93.4 % can be achieved with a total cost of 456,000 \$/year. The increase in efficiency is greatly acknowledged by the increase in the cost which becomes a challenge in the practical application.

The result indicates that baffle cut and baffle spacing are important parameters when the heat exchanger is subjected to cost minimization as shown in Fig. 7(a) and (b). The total minimum cost of the system was 72,000 \$/year and 75,400 \$/year when the baffle cut and baffle spacing was 0.2 m and 0.05 m; whereas the total cost was 275,000 \$/year and 269,000 \$/year when the geometrical variables were maximum as 0.35 and 0.5 m. The increase in the total cost of the system was subject to the increase in the overall heat transfer area of the heat exchanger.

5.2. Parametric analysis – tube side design variables

The effect of tube side design variables, tube layout, tube outside diameter, number of tube passes and number of tubes on the heat exchanger efficiency and the total cost of the heat exchanger is presented in Fig. 8. The effect of tube layout on the total cost and heat

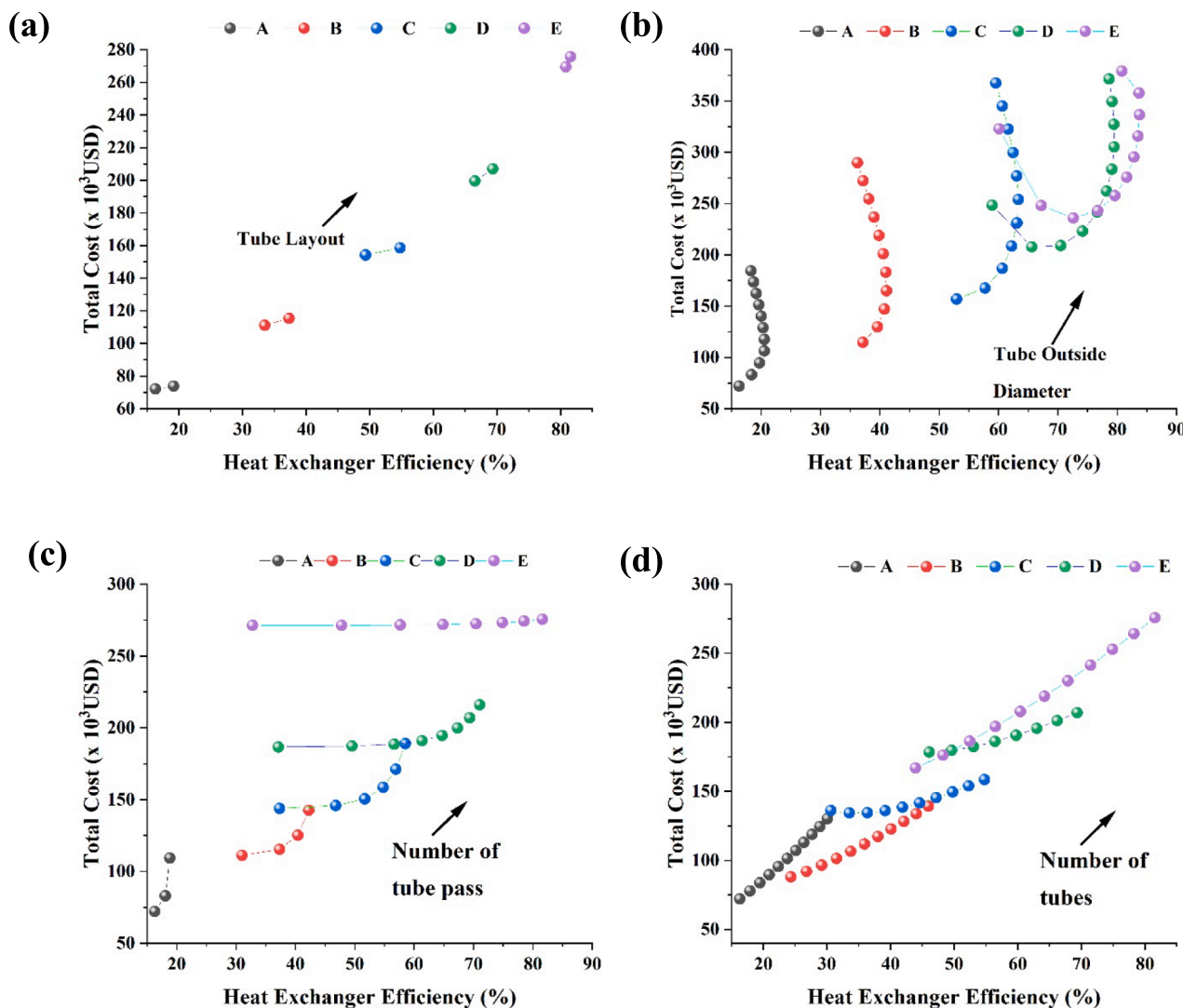


Fig. 8. Results of parametric analysis for the variables of tube side.

exchanger efficiency is shown in Fig. 8(a). It can be observed from the figure that with rise in tube layout for any design point (i.e. A–E) results in a corresponding increase in both objectives. However, the percentage increase in total cost is more as compared to the increase in heat exchanger efficiency. In addition, the percentage increases in both objectives are elevated at higher tube layouts. Overall, the effect of tube layout is profound in minimizing the total cost of the system and the optimum tube layout was 30° as shown in Fig. 8(a). The tube outside diameter was varied from 15 mm to 51 mm and the increase in the tube outside diameter resulted in increased heat transfer area and correspondingly reduced pressure drop in the tube flow. The total cost increased from 72,000 \$/year to 379,000 \$/year with the increase in tube outside diameter from 15 mm to 51 mm, whereas the heat exchanger efficiency increased from 16.3 % to 80.7 %, as shown in Fig. 8 (b).

The variation in the number of tubes passes from 1 to 8 resembles an increase in the total cost of the system at lower efficiency as represented in Fig. 8(c). However, the change in the total cost is marginal when the heat exchanger is operated for higher thermal efficiency. At the optimal point E, the variation in the total cost is barely 1.6 % whereas the heat exchanger efficiency varied from 32.8 % to 81.6 % between the minimum and maximum limits. The effect of the number of tubes is profound on the thermal efficiency and at the same time it impacts the total cost of

the heat exchanger as shown in Fig. 8(d). The obvious reason for increasing the heat transfer area directly influences the heat transfer and subsequently the heat exchanger efficiency. For the minimum total cost, at point A, the variation in the heat exchanger efficiency and the total cost between the maximum and minimum limits is 84 % and 80 %, respectively. However, for the maximum heat exchanger efficiency, at the point E, the variation in the objective functions is 85 % and 65 %, respectively.

5.3. Population distribution – shell side design variables

Fig. 9 shows the distribution of Pareto points for the decision variables of the shell side of the heat exchanger. The distribution of the optimal points of baffle cut, baffle spacing and shell diameter is presented between the upper and lower bounds. The distribution of the baffle cut between the bounds is congregated at around 20 % signifying the monotonous effect on the objective functions presented in Fig. 9(a). The results in Fig. 9(b) and (c) show that the effect of baffle spacing and the shell diameter is profound and the distribution is scattered widely between the bounds. It signifies that the effect of design variables in obtaining the optimum value significant.

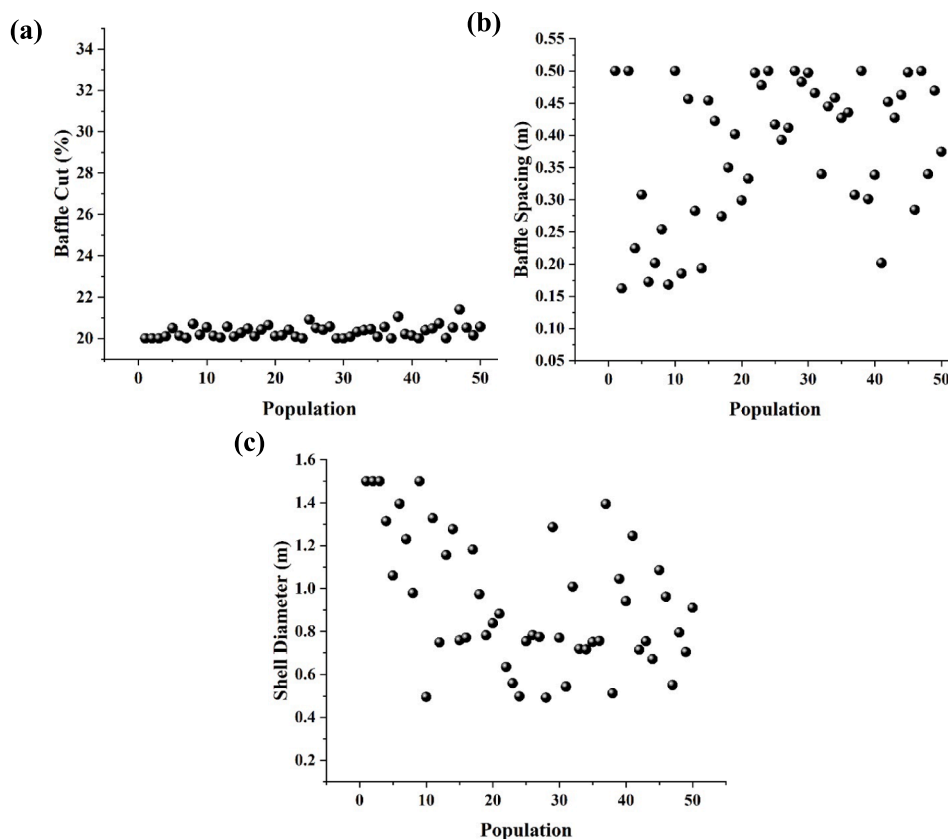


Fig. 9. Distribution of shell-side decision variables.

5.4. Population distribution – tube side design variables

Fig. 10 shows the distribution of Pareto points for the decision variables of the tube side of the heat exchanger. The distribution of the optimal points of tube layout, tube outside diameter, number of tube passes and the number of tubes in the heat exchanger is presented between the upper and lower bounds.

The distribution of tube layout across the lower and upper bound is monotonous and it is evident from Fig. 10(a) that the optimum values of the objective functions are obtained at 30° tube layout. The distribution of the tube outside diameter as shown in Fig. 10(b) is scattered across the bounds, however, 0.035 mm was the maximum limit of the tube diameter to get the optimum values of the objective functions. The number of tube passes and the number of tubes were scattered across the bounds to get the optimum value of the objective functions as shown in Fig. 10(c) and (d). The scattered distribution resembles the variation of the objective function in achieving the minimum total cost and the maximum thermal efficiency.

6. Conclusions

In this study, a water-water segmental baffle shell and tube exchanger was modelled by the Kern method and analyzed from an energy-economic point of view. The system consisted of two centrifugal pumps and one shell and tube heat exchanger, whose application is to heat cold water by a hot water flow. During the water-to-water heat transfer, the exergy destruction, heat exchanger efficiency, capital cost, and operational cost of various streams were calculated through energy-economic analysis. System optimization was performed to minimize the total cost per year and maximize the heat exchanger efficiency. A heat transfer search algorithm was used to optimize the system and multiple Pareto optimal points were obtained as the result. With the help of the TOPSIS decision-making criteria, the optimum point was selected from

the Pareto front, and the optimum point indicated the values of seven decision variables, i.e., shell diameter, tube outside diameter, baffle cut, baffle spacing, number of tube pass, number of tubes and tube layout. Following are the important findings of the study.

- The optimum geometric configuration for the heat exchanger as selected by TOPSIS criteria can yield the heat exchanger efficiency of 59.9 % at a total cost of 175,000 \$/year. Among the variables on the shell side, shell diameter profoundly affects the objective functions as a maximum efficiency of 93.4 % can be achieved with a total cost of 456,000 \$/year.
- The result also indicates that baffle cut and baffle spacing are important parameters when the heat exchanger is subjected to cost minimization.
- Similarly, the effect of tube layout is profound in minimizing the total cost of the system and the optimum tube layout was 30°. A triangular pitch is observed to be more effective than a square pitch tube layout.
- The effect of the number of tubes is profound on the thermal efficiency and at the same time it impacts the total cost of the heat exchanger
- The scattered distribution of baffle spacing, shell diameter, tube outside diameter, number of tube passes and number of tubes represent profound effects on obtaining optimal heat exchanger efficiency and total cost. Whereas, the effect of tube layout and baffle cut is monotonous on the system performance.

CRedit authorship contribution statement

Parth Prajapati: Writing – original draft, Validation, Formal analysis, Data curation. **Bansi D. Raja:** Writing – original draft, Formal analysis, Data curation. **Vivek Patel:** Writing – review & editing, Project administration, Investigation. **Hussam Jouhara:** Writing – review &

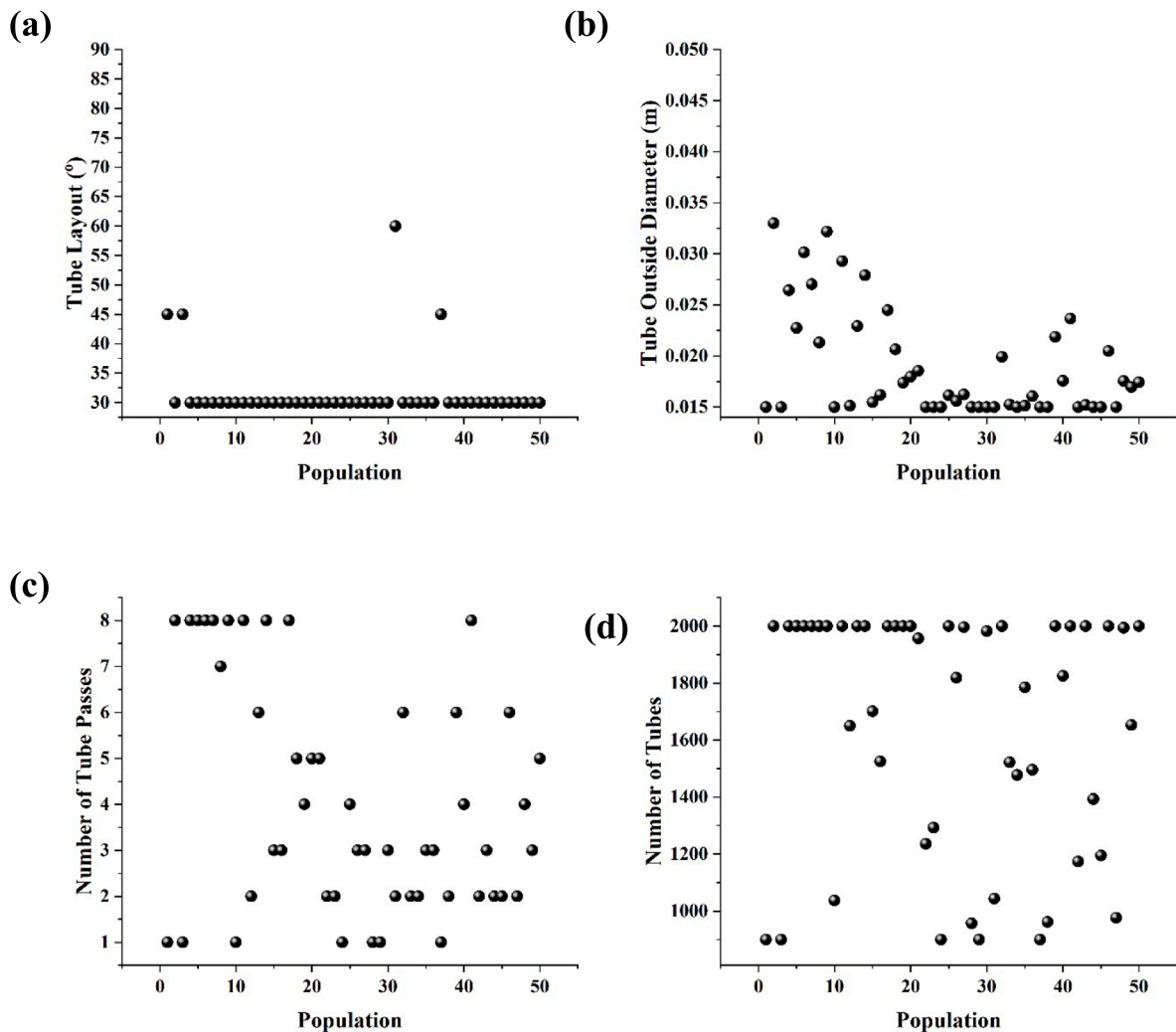


Fig. 10. Distribution of tube-side decision variables.

editing.

Declaration of competing interest

The authors declare that they have no known competing financial interests or personal relationships that could have appeared to influence the work reported in this paper.

Acknowledgement

The work was done as part of the collaboration between *Pandit Deendayal Energy University* and the Heat Pipe and Thermal Management Research Group at Brunel University London, UK.

Data availability

No data was used for the research described in the article.

References

- [1] P. Catrini, A. Cipollina, G. Micale, A. Piacentino, A. Tamburini, Exergy analysis and thermo-economic cost accounting of a Combined Heat and Power steam cycle integrated with a Multi Effect Distillation-Thermal Vapour Compression desalination plant, *Energ. Convers. Manage.* 149 (2017) 950–965, <https://doi.org/10.1016/J.ENCONMAN.2017.04.032>.
- [2] V.K. Patel, B.D. Raja, P. Prajapati, L. Parmar, H. Jouhara, An investigation to identify the performance of cascade refrigeration system by adopting high-temperature circuit refrigerant R1233zd (E) over R161, *Int. J. Thermofluids* 17 (December 2022) (2023) 100297, <https://doi.org/10.1016/j.ijft.2023.100297>.
- [3] P. Prajapati, V. Patel, H. Jouhara, An efficient optimization of an irreversible Ericsson refrigeration cycle based on thermo-ecological criteria, *Therm. Sci. Eng. Prog.* (2022) 101381, <https://doi.org/10.1016/J.TSEP.2022.101381>.
- [4] C. Gulenoglu, F. Akturk, S. Aradag, N. Sezer Uzol, S. Kakac, Experimental comparison of performances of three different plates for gasketed plate heat exchangers, *Int. J. Therm. Sci.* 75 (2014) 249–256, <https://doi.org/10.1016/J.IJTHEMALSCI.2013.06.012>.
- [5] P. Prajapati, V. Patel, Multi-objective optimization of CuO based organic Rankine cycle operated using R245ca, in: *E3S Web of Conferences*, 2019, <https://doi.org/10.1051/e3sconf/201911600062>.
- [6] S.K. Gupta, H. Verma, N. Yadav, A review on recent development of nanofluid utilization in shell & tube heat exchanger for saving of energy, *Mater. Today Proc.* 54 (2022) 579–589, <https://doi.org/10.1016/j.matpr.2021.09.455>.
- [7] M. Miansari, M.A. Valipour, H. Arasteh, D. Toghraie, Energy and exergy analysis and optimization of helically grooved shell and tube heat exchangers by using Taguchi experimental design, *J. Therm. Anal. Calorim.* 139 (5) (2020) 3151–3164, <https://doi.org/10.1007/S10973-019-08653-3/FIGURES/16>.
- [8] J.M. Ponce-Ortega, M. Serna-González, A. Jiménez-Gutiérrez, Use of genetic algorithms for the optimal design of shell-and-tube heat exchangers, *Appl. Therm. Eng.* 29 (2–3) (2009) 203–209, <https://doi.org/10.1016/J.APPLTHERMALENG.2007.06.040>.
- [9] H. Sadeghzadeh, M.A. Ehyaei, M.A. Rosen, Techno-economic optimization of a shell and tube heat exchanger by genetic and particle swarm algorithms, *Energ. Convers. Manage.* 93 (2015) 84–91, <https://doi.org/10.1016/J.ENCONMAN.2015.01.007>.
- [10] H. Hajabdollahi, M. Naderi, S. Adimi, A comparative study on the shell and tube and gasket-plate heat exchangers: the economic viewpoint, *Appl. Therm. Eng.* 92 (2016) 271–282, <https://doi.org/10.1016/J.APPLTHERMALENG.2015.08.110>.

- [11] H. Hajabdollahi, P. Ahmadi, I. Dincer, Exergetic optimization of shell-and-tube heat exchangers using NSGA-II, 33(7) (2012) 618–628. doi: 10.1080/01457632.2012.630266.
- [12] D.K. Mohanty, Gravitational search algorithm for economic optimization design of a shell and tube heat exchanger, *Appl. Therm. Eng.* 107 (2016) 184–193, <https://doi.org/10.1016/j.applthermaleng.2016.06.133>.
- [13] S.V. Dhavle, A.J. Kulkarni, A. Shastri, I.R. Kale, Design and economic optimization of shell-and-tube heat exchanger using cohort intelligence algorithm, *Neural Comput. Appl.* 30 (1) (2018) 111–125, <https://doi.org/10.1007/s00521-016-2683-z>.
- [14] K. Wang, G. Sun, Y. Wang, X. Dai, W. Chen, Z. Liu, CFD simulation and optimization study on the shell side performances of a plate and shell heat exchanger with double herringbone plates, *Therm. Sci. Eng. Prog.* 43 (2023) 101931, <https://doi.org/10.1016/j.tsep.2023.101931>.
- [15] S. Han, X. Li, Z. Liu, B. Zhang, C. He, Q. Chen, Thermal-economic optimization design of shell and tube heat exchanger using an improved sparrow search algorithm, *Therm. Sci. Eng. Prog.* 45 (2023) 102085, <https://doi.org/10.1016/j.tsep.2023.102085>.
- [16] A.C. Caputo, A. Federici, P.M. Pelagagge, P. Salini, On the selection of design methodology for shell-and-tube heat exchangers optimization problems, *Therm. Sci. Eng. Prog.* 34 (2022) 101384, <https://doi.org/10.1016/j.tsep.2022.101384>.
- [17] N. Biçer, T. Engin, H. Yaşar, E. Büyükkaya, A. Aydın, A. Topuz, Design optimization of a shell-and-tube heat exchanger with novel three-zonal baffle by using CFD and taguchi method, *Int. J. Therm. Sci.* 155 (2020) 106417, <https://doi.org/10.1016/j.jithermalsci.2020.106417>.
- [18] D. Thondiyil, S. Kizhakke Kodakkattu, Optimization of a shell and tube heat exchanger with staggered baffles using Taguchi method, *Mater. Today: Proc.* 46 (2021) 9983–9988, <https://doi.org/10.1016/j.matpr.2021.04.092>.
- [19] R. Khosravi, A. Khosravi, S. Nahavandi, H. Hajabdollahi, Effectiveness of evolutionary algorithms for optimization of heat exchangers, *Energ. Convers. Manage.* 89 (2015) 281–288, <https://doi.org/10.1016/j.enconman.2014.09.039>.
- [20] W.H. Saldanha, G.L. Soares, T.M. Machado-Coelho, E.D. Dos Santos, P.I. Ekel, Choosing the best evolutionary algorithm to optimize the multiobjective shell-and-tube heat exchanger design problem using PROMETHEE, *Appl. Therm. Eng.* 127 (2017) 1049–1061, <https://doi.org/10.1016/j.applthermaleng.2017.08.052>.
- [21] S. Mohapatra, D.K. Das, A.K. Singh, An optimal plate-fin heat exchanger design using opposition-based Orthogonal Learning Kho-Kho Optimization algorithm, *Prog. Nucl. Energy* 177 (2024) 105416, <https://doi.org/10.1016/j.pnucene.2024.105416>.
- [22] M.A. Jamil, T.S. Goraya, M.W. Shahzad, S.M. Zubair, Exergoeconomic optimization of a shell-and-tube heat exchanger, *Energ. Convers. Manage.* 226 (2020) 113462, <https://doi.org/10.1016/J.ENCONMAN.2020.113462>.
- [23] N. Li, et al., Analysing thermal-hydraulic performance and energy efficiency of shell-and-tube heat exchangers with longitudinal flow based on experiment and numerical simulation, *Energy* 202 (2020) 117757, <https://doi.org/10.1016/j.energy.2020.117757>.
- [24] S.H.L.A.P. Kakac, Heat exchangers: selection, rating, and thermal design, 36(01) (1998). doi: 10.5860/choice.36-0348.
- [25] G. Towler, R.A.Y. Sinnott, *Chemical engineering design: principles, practice and economics of plant and process design*, 2013. doi: 10.1016/b978-0-08-096659-5.00022-5.
- [26] M.S. Peters, K.D. Timmerhaus, *Plant design and economics for chemical engineers*, 1991.
- [27] M. Mehdizadeh-Fard, F. Pourfayaz, A. Maleki, Exergy analysis of multiple heat exchanger networks: an approach based on the irreversibility distribution ratio, *Energy Rep.* 7 (2021) 174–193, <https://doi.org/10.1016/J.EGYR.2020.11.166>.
- [28] R. Mukherjee, Effectively design shell-and-tube heat exchangers, *Chem. Eng. Prog.* 94 (2) (1998).
- [29] Z. Rogala, P. Kolasinski, Exergy analysis of fluidized desiccant cooling system, *Entropy* 21(8) (2019) 757. doi: 10.3390/E21080757.
- [30] P. Prajapati, V. Patel, B.D. Raja, H. Jouhara, Multi objective ecological optimization of an irreversible Stirling cryogenic refrigerator cycle, *Energy* 274 (Jul. 2023) 127253, <https://doi.org/10.1016/J.ENERGY.2023.127253>.
- [31] G. Tsatsaronis, Definitions and nomenclature in exergy analysis and exergoeconomics, *Energy* 32 (4) (2007) 249–253, <https://doi.org/10.1016/J.ENERGY.2006.07.002>.
- [32] I.L. Paniagua, J.R. Martín, C.G. Fernandez, Á.J. Álvaro, R.N. Carlier, A new simple method for estimating exergy destruction in heat exchangers, *Entropy* 15 (2013) 474–489, <https://doi.org/10.3390/E15020474>.
- [33] V.H. Iyer, S. Mahesh, R. Malpani, M. Sapre, A.J. Kulkarni, Adaptive Range Genetic Algorithm: a hybrid optimization approach and its application in the design and economic optimization of Shell-and-Tube Heat Exchanger, *Eng. Appl. Artif. Intel.* 85 (2019) 444–461, <https://doi.org/10.1016/J.ENGAPPAL.2019.07.001>.
- [34] A.C. Caputo, P.M. Pelagagge, P. Salini, Heat exchanger design based on economic optimisation, *Appl. Therm. Eng.* 28 (10) (2008) 1151–1159, <https://doi.org/10.1016/J.APPLTHERMALENG.2007.08.010>.
- [35] P.P. Prajapati, V.K. Patel, Comparative analysis of nanofluid-based Organic Rankine Cycle through thermoeconomic optimization, 2019. doi: 10.1002/hj.21528.
- [36] H.P. Loh, J. Lyons, I.I.I. Charles, W. White, *Process Equipment Cost Estimation, Final Report, National Energy Technology Laboratory, US Department of Energy*, no. January, p. Medium: ED; Size: 410 Kilobytes pages, 2002.
- [37] Y.M. El-Sayed, Designing desalination systems for higher productivity, *Desalination* 134 (1–3) (2001) 129–158, [https://doi.org/10.1016/S0011-9164\(01\)00122-9](https://doi.org/10.1016/S0011-9164(01)00122-9).
- [38] V.K. Patel, V.J. Savsani, Heat transfer search (HTS): a novel optimization algorithm, *Inf. Sci.* 324 (2015) 217–246, <https://doi.org/10.1016/J.INS.2015.06.044>.
- [39] B.D. Raja, R.L. Jhala, V. Patel, Many-objective optimization of cross-flow plate-fin heat exchanger, *Int. J. Therm. Sci.* 118 (2017) 320–339, <https://doi.org/10.1016/J.IJTHEMALSCI.2017.05.005>.
- [40] B.D. Raja, R.L. Jhala, V. Patel, Thermal-hydraulic optimization of plate heat exchanger: a multi-objective approach, *Int. J. Therm. Sci.* 124 (2018) 522–535, <https://doi.org/10.1016/J.IJTHEMALSCI.2017.10.035>.
- [41] C.-L. Hwang, K. Yoon, *Multiple Attribute Decision Making*, vol. 186. in *Lecture Notes in Economics and Mathematical Systems*, vol. 186, Springer Berlin Heidelberg, Berlin, Heidelberg, 1981. doi: 10.1007/978-3-642-48318-9.
- [42] P. Prajapati, V. Patel, B.D. Raja, H. Jouhara, Energy-exergy-economic-environmental (4E) analysis and multi-objective optimization of a cascade refrigeration system, *Therm. Sci. Eng. Prog.* 54 (2024) 102793, <https://doi.org/10.1016/j.tsep.2024.102793>.